PAPER • OPEN ACCESS

Optimization of 3D printing parameters for enhanced tensile properties in continuous carbon fiber reinforced PLA composites

To cite this article: Fidan Bilir Kilinc *et al* 2025 *Mater. Res. Express* **12** 045302

Materials Research Express

PAPER

Optimization of 3D printing parameters for enhanced tensile properties in continuous carbon fiber reinforced PLA composites

Fidan Bilir Kilinc[1], **Turker Turkoglu**[2], **Saadet Guler**[3] and **Ahmet Cagri Kilinc**[4]

[1] Ege University, Department of Textile Engineering, Graduate School of Natural and Applied Sciences, Izmir, Turkey
[2] Balıkesir University, Department of Mechanical Engineering, Balıkesir, Turkey
[3] Izmir Katip Çelebi University, Department of Metallurgical and Materials Engineering, Izmir, Turkey
[4] Osmaniye Korkut Ata University, Department of Mechanical Engineering, Osmaniye, Turkey

E-mail: turker.turkoglu@balikesir.edu.tr

OPEN ACCESS

RECEIVED
1 February 2025

REVISED
14 March 2025

ACCEPTED FOR PUBLICATION
26 March 2025

PUBLISHED
22 April 2025

Keywords: additive manufacturing, continuous carbon fiber, fused deposition modeling, process optimization, taguchi method, tensile properties

Abstract

In this study, the effect of 3D printing process parameters, specifically line width and layer thickness, on the tensile properties of continuous carbon fiber-reinforced PLA composites fabricated via the Fused Filament Fabrication (FFF) method was investigated. The incorporation of continuous carbon fibers into the PLA matrix aims to enhance the mechanical performance of the printed composites, overcoming the inherent limitations of polymer-based additive manufacturing. The Taguchi method was employed to optimize the process parameters, enabling a systematic evaluation of their influence on tensile strength. An L9 orthogonal array was used to design the experiments, and the Signal-to-Noise (S/N) ratio was analyzed to determine the optimal parameter combination. The results demonstrate that line width and layer thickness significantly affect the tensile performance of printed composites, with narrower line widths (1.0 mm) and thinner layers (0.2 mm) yielding the highest tensile strength (291.3 MPa). Statistical analysis using Analysis of Variance (ANOVA) revealed that line width contributes 58.65% to the overall mechanical performance, making it the most influential factor, followed by layer thickness (33.55%). Microstructural analyses further confirmed that optimized printing parameters improve fiber alignment, enhance interlayer bonding, and minimize void formation. These findings highlight the crucial role of process optimization in maximizing the mechanical properties of FFF-printed continuous carbon fiber reinforced polymer (CFRP) composites, offering insights into achieving high-performance and lightweight structural components.

1. Introduction

Additive manufacturing (AM), widely known as 3D printing, has emerged as a transformative technology in the manufacturing sector due to its ability to produce complex geometries, reduced material wastage, and cost-effective small-batch production [1]. Among the various AM techniques, Fused Filament Fabrication (FFF) has gained significant attention for fabricating thermoplastic-based components, particularly due to its simplicity, affordability, and adaptability for a wide range of materials [2]. Despite these advantages, the mechanical properties of FFF-produced components often lag behind those manufactured using conventional methods, primarily due to issues such as weak interlayer adhesion and void formation [3]. Addressing these limitations has become a focal point for researchers, with one promising avenue being the incorporation of reinforcing fibers to enhance mechanical performance [4].

Continuous carbon fiber reinforced polymer (CFRP) have demonstrated exceptional potential in overcoming the mechanical limitations of FFF-printed parts [5]. These composites leverage the high strength-to-weight ratio and stiffness of continuous carbon fibers, which, when embedded into a thermoplastic matrix such as polylactic acid (PLA), yield components suitable for applications in aerospace, automotive, and

structural engineering [6, 7]. PLA, a biodegradable and environmentally friendly thermoplastic, further enhances the appeal of these composites by aligning with global sustainability goals [8]. The integration of continuous fibers has shown to significantly improve tensile strength and modulus, making it a preferred choice for advanced composite fabrication [9].

Process parameters, such as line width and layer thickness, play a crucial role in determining the mechanical properties of FFF-printed CFRP components [3]. Variations in these parameters influence fiber alignment, interlayer bonding, and overall part density, directly impacting tensile properties. For instance, optimizing line width can enhance the fiber-matrix interface, while layer thickness adjustments affect the interlaminar strength and porosity [10]. Previous studies have emphasized the need for systematic exploration of these parameters to achieve composites with tailored mechanical properties [6]. One effective approach to achieve such optimization is the application of the Taguchi method, which provides a robust statistical framework for analyzing and optimizing process parameters. It becomes possible to systematically identify the optimal combination of line width and layer thickness by employing this method, minimizing variability and enhancing the mechanical performance of the composites. Optimization plays a crucial role in additive manufacturing, where small changes in process parameters can lead to significant variations in mechanical properties and production quality [11]. Effective optimization not only improves part performance but also reduces material waste, production time, and costs, making it an integral aspect of advancing additive manufacturing technologies [9, 12].

Ponsuriyaprakash *et al* [13] conducted a study on the mechanical, thermal, and morphological properties of Acrylonitrile Butadiene Styrene (ABS) composites reinforced with cellulose fibers at varying weight fractions. The incorporation of 20% cellulose fibers into the ABS matrix resulted in a 37% improvement in tensile strength compared to pure ABS. Thermal analyses demonstrated enhanced thermal stability with cellulose reinforcement, highlighting its efficacy as a reinforcing filler. Morphological investigations revealed improved fiber-matrix bonding and detailed fracture mechanisms. This study concludes that cellulose-reinforced ABS composites offer superior mechanical performance and environmental sustainability, making them a promising candidate for lightweight and durable material applications. Yu *et al* [14] examined the impact of thermal annealing on the physical, thermal, and mechanical properties of polymer parts produced via material extrusion 3D printing, focusing on semi-crystalline and amorphous polymers. Samples were annealed at temperatures exceeding their glass transition temperature (T_g), specifically at 60 °C, 110 °C, and 150 °C, for varying durations. Results showed that thermal annealing significantly enhanced flexural strength and Young's modulus for semi-crystalline polymers, achieving up to a 10% improvement due to crystallinity development. However, dimensional changes, such as strand thickness expansion and shrinkage in other directions, were observed. These morphological changes diminished local tensile deformation performance, particularly for amorphous parts, where mechanical properties degraded by up to 25%. The study underscores the dual role of annealing, offering improvements in mechanical integrity for semi-crystalline materials while highlighting potential drawbacks for amorphous structures, emphasizing the need for temperature and duration optimization. Sethu *et al* [15] explored a novel hybrid fabrication approach integrating additive manufacturing (AM) and compression molding to produce bamboo-reinforced polylactic acid (PLA) composites. Using FFF, PLA was deposited onto bamboo woven mats, followed by compression molding to create composite sheets with improved thickness and properties. The effect of FFF nozzle temperature on the mechanical, thermal, and microstructural characteristics of the composites was systematically analyzed. Results revealed that increasing the nozzle temperature enhanced interfacial adhesion, reduced porosity, and significantly improved tensile, flexural, and impact strength. Microstructural evaluations identified fiber breakage and interface decohesion as primary failure mechanisms. The study concludes that bamboo-PLA composites offer superior mechanical performance and highlights the potential of optimizing AM parameters for sustainable material applications. Prajapati *et al* [16] investigated the impact energy absorption and fracture mechanisms of continuous fiberglass-reinforced polymer composites produced via FFF. Key parameters such as build orientation, fiber stacking sequence, and fiber angle were analyzed using Charpy impact testing, with composites reinforced by standard fiberglass and high-strength high-temperature (HSHT) fiberglass. Results revealed that the XYZ build orientation, B-type stacking sequence, and 0°/90° fiber angles provided optimal impact energy absorption, with HSHT fiberglass outperforming standard fiberglass. Morphological analysis identified fiber pullout and bonding defects as primary failure mechanisms. The findings of this study have significant practical implications for aerospace, automotive, and structural engineering applications, where lightweight, high-strength materials are essential. By optimizing line width and layer thickness using the Taguchi method, this study enables precise control of mechanical properties in FFF-printed PLA-CFRP composites, leading to improved structural performance. In aerospace, the optimized composites enhance strength-to-weight ratio, making them ideal for aircraft components and unmanned aerial vehicle (UAV) structures. In the automotive sector, the ability to tailor mechanical properties supports the production of lightweight, crash-resistant components, contributing to fuel efficiency and enhanced safety. Similarly, in structural engineering, optimized CFRP composites can be

utilized in seismic retrofitting, bridge reinforcements, and load-bearing structures, offering superior mechanical durability and corrosion resistance. The study demonstrates that precise process parameter refinement in FFF manufacturing can lead to customizable, high-performance composite solutions, reducing material waste and enabling cost-effective, application-driven fabrication.

This study focuses on the effect of line width and layer thickness on the tensile properties of PLA-CFRP composites fabricated using FFF. The work aims to uncover insights into their influence on mechanical performance by systematically varying these production parameters. While previous studies have investigated CFRP composites in additive manufacturing, limited research has systematically examined the combined effects of line width and layer thickness on tensile properties, particularly using a structured statistical optimization approach. This study addresses this gap by employing the Taguchi method to optimize these parameters, ensuring improved reproducibility and mechanical performance in FFF-printed CFRP components. The findings are expected to contribute to the optimization of FFF process parameters, advancing the production of high-performance composite components for engineering applications. Additionally, the integration of the Taguchi method within this study will offer a structured and efficient approach to refining the process, ensuring reproducible and superior outcomes.

2. Materials and methods

2.1. Materials

Poly lactic acid (PLA) (ESUN) filament with tensile strength of 63 MPa and tensile modulus of 1.9 GPa was used as a polymeric matrix material of composites. 1K continuous carbon fiber tow with tensile strength of 3500 MPa and tensile modulus of 230 GPa, containing 1000 elementary fibers was used as reinforcement.

2.2. 3D printing of continuous fiber reinforced composites

Commercial hot-end systems available on the market are generally standardized for 3D printing of thermoplastic filaments with a diameter of 1.75 mm. These hot-end systems are generally used to guide and print a single filament. When such hot-end systems are used for continuous fiber reinforcement, the reinforcement fiber is generally fed into the system from the same point as the polymeric filament. In this case, relatively high friction forces occur between the polymeric filament which generates tension force on the reinforcement fiber. Due to the transfer of this force to the deposited fiber, problems such as damage or break of the fibers were observed during the printing trials with commercial hot-end systems such as E3DV6. For this reason, in this study, the polymeric filament and the reinforcement fiber were fed into the system separately. For this purpose, a heating block with a straight fiber path was produced from aluminum alloy due to its relatively high thermal conductivity. A stainless-steel dispensing needle was placed on the aluminum heating block to create the straight fiber path. The heatsink and heat break parts of commercial E3DV6 hot-end were also mounted on the heating block to feed PLA filament, which was used as the matrix material. The cross-section of extruder and nozzle structure are given schematically in figure 1.

The 3D printing process of composites was carried out using a desktop FFF printer. The prepared hot-end system with a capable of nozzle impregnation was mounted on the 3D printer. The printing parameters such as nozzle temperature and printing speed were fixed at 210 °C and 10 mm s^{-1} respectively fixed printing parameters are given in table 1.

Layer thickness and line width parameters were investigated within the scope of the study as these parameters affect the continuous carbon fiber reinforcement fraction in the composites. Layer thickness and line width parameters which were determined based on the printing trials were given in table 2. The overall process flowchart was shown in figure 2.

2.3. Characterization

2.3.1. Characterization of materials

Surface of the fibers was examined by scanning electron microscope (SEM) (ZEISS, EVO HD15) in addition to the determination of fiber diameter. Thermal behavior of poly lactic acid (PLA) was examined by using thermogravimetric analysis (TGA) (PerkinElmer, STA 8000). Samples were heated from room temperature to 600 °C with a heating ramp of 10 °C min^{-1} under nitrogen atmosphere. X-ray diffraction (XRD) measurements of PLA and carbon fibers were carried out by using x-ray diffractometer (BRUKER, D2 PHASER) with Cu—Kα radiation (λ-Kα1 = 1.54 Å). Samples were scanned in (2θ) range of 10°–80° with a scan speed of 4° min^{-1}.

2.3.2. Characterization of composites

3D printed unidirectional composite specimens with different printing parameters of layer thickness and line width, were cut and cold mounted by using epoxy resin for preparation of cross-sectional optical investigations.

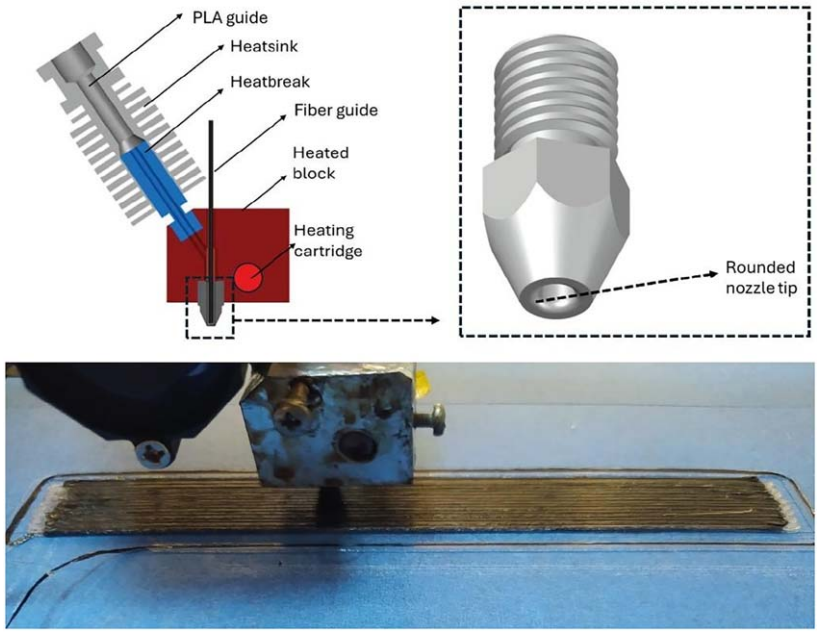

Figure 1. The cross-section of extruder and nozzle structure.

Table 1. Fixed 3D printing parameters.

Parameter	Value
Printing temperature	210 °C
Bed temperature	Room temperature
Printing speed	10 mm s^{-1}
Infill angle	0 ° (unidirectional)
Infill density	100%

Table 2. Variable 3D printing parameters of composites.

Label of specimens	Line width (mm)	Layer thickness (mm)
2_06	2	0.6
2_04	2	0.4
2_02	2	0.2
1.5_06	1.5	0.6
1.5_04	1.5	0.4
1.5_02	1.5	0.2
1_06	1	0.6
1_04	1	0.4
1_02	1	0.2

The prepared samples were ground by using 80 to 1200 grit sandpapers and prepared specimens were investigated under an optical microscope (Leica, DM 2500).

The fiber volume fractions of the composites were determined by calculating the fiber to sample cross-sectional ratio based on the study of Waterbury and Drzal [17]. The same cross-sectional profile extending across the length of the bar is assumed in this method and therefore the area fraction and volume fraction are considered to be the same [18]. Therefore, fiber volume fractions of composites 3D printed with different line width and layer thickness parameters were calculated as follows:

$$V_f = \frac{Fibers\ per\ cross\ section \times Area\ per\ fiber}{Cross\ section\ of\ specimen} \quad (1)$$

where the V_f refers to fiber volume fraction. Since 1K fiber tow was used in the study and the number of deposited lines forming the sample was known depending on the printing parameters of the samples, the fiber

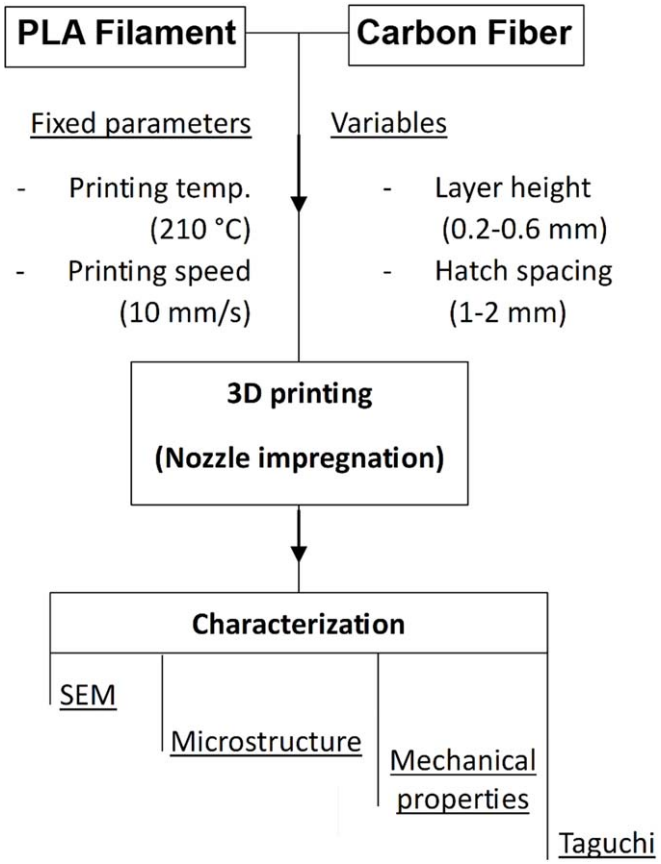

Figure 2. The process flowchart.

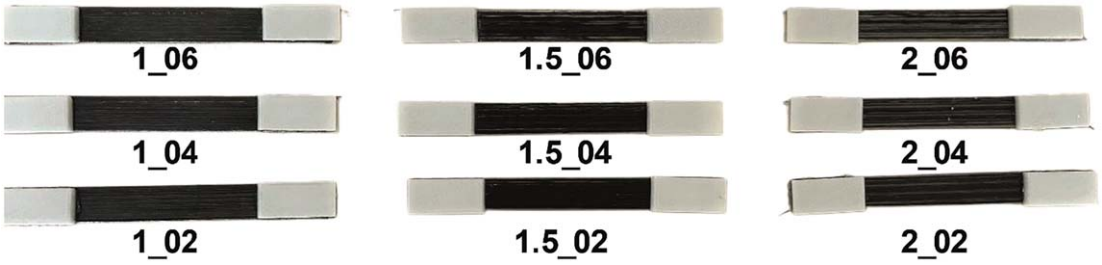

Figure 3. Image of tensile testing specimens.

per cross-section in the samples was calculated as follows:

$$Fibers\ per\ cross\ section = 1000 \times deposited\ line\ count \quad (2)$$

Mechanical properties of 3D printed unidirectional composite specimens were determined by tensile testing. Specimens with dimensions of 150 mm * 12 mm * 2.4 mm (printing directions: x * y * z) were printed by using continuous path design. 3D printed tabs were adhesively bonded to the ends of the specimens to reduce the load transferred from grips. Samples were tested at a crosshead speed of 2 mm s^{-1} by using a universal tensile testing machine (Zwick/Roell, Z250). Image of tensile testing specimens 3D printed with different layer thickness and layer thickness values are shown in figure 3. Fracture surface morphologies of composites were examined by using scanning electron microscope (SEM). Sputter coating was applied to the specimens to prevent electron charging problems during SEM investigations.

2.4. Taguchi analysis

In this study, the Taguchi method was employed to optimize the process parameters for producing continuous carbon fiber-reinforced PLA composites by the FFF method. The Taguchi method, a widely used robust design

Table 3. The process parameters and levels.

		Levels		
Factors	Units	−1	0	+1
Line width (mm)	mm	1.0	1.5	2.0
Layer thickness (mm)	mm	0.2	0.4	0.6

optimization technique, was utilized to systematically investigate the influence of key printing parameters on the tensile performance of the composites. This method enables efficient optimization by reducing the number of experimental runs while enhancing process stability and product quality.

Taguchi's orthogonal array-based experimental design approach allows for systematic control of input factors, minimizing variability and improving the repeatability of experimental outcomes. As highlighted by Mohammed *et al* [19] the Taguchi method establishes a strong connection between input and output variables while reducing the total number of required trials, making it an effective approach for process optimization in additive manufacturing

Generally, there are three types of performance characteristics in the analysis of the S/N ratio:

Larger-the-Better: Applied when maximizing the response variable is the objective, such as tensile strength or hardness. The S/N ratio is given by equation (3):

$$\frac{S}{N} = -10\log\left(\frac{1}{n} * \sum_{k}^{n} 1/y_k^2\right) \tag{3}$$

The Larger-the-Better criterion was selected as the objective function, with tensile strength as the primary response variable. This approach is particularly suitable when the aim is to maximize a desired property, ensuring that the selected process parameters lead to the highest possible mechanical performance. The influence of variations in process conditions on tensile strength was analyzed by employing the Signal-to-Noise (S/N) ratio for the Larger-the-Better characteristic, which minimizes the impact of experimental noise and improving reproducibility. The S/N ratio for the Larger-the-Better approach, which was adopted in this study to maximize the tensile strength of the composites. In this study, an L9 orthogonal array was selected to evaluate the effects of key process parameters, including line width and layer thickness, on the tensile properties of continuous carbon fiber-reinforced PLA composites produced via FFF method. Each parameter was analyzed at three different levels to systematically assess their impact on mechanical performance. The signal-to-noise (S/N) ratio was calculated for each experimental condition using the Larger-the-Better approach to identify the optimal parameter combination that maximizes tensile strength while minimizing variability and process-induced defects. This structured approach ensures a robust analysis of the relationship between process parameters and mechanical properties, facilitating the development of optimized printing conditions for high-performance composites. Table 3 presents the selected process parameters, and their corresponding levels used in this study to evaluate the effect of 3D printing conditions on the tensile properties of continuous carbon fiber-reinforced PLA composites.

The experimental design used in this study follows an orthogonal array approach to systematically evaluate the effects of line width and layer thickness on the mechanical properties of continuous carbon fiber-reinforced PLA composites produced via FFF method. The selected process parameters were investigated across nine experimental runs, as shown in table 4, allowing for a comprehensive analysis of their interactions and individual contributions to tensile strength. An optimized parameter set for maximizing tensile properties was obtained by utilizing the Taguchi method to quantify the influence of process parameters using the signal-to-noise (S/N) ratio.

3. Results

3.1. Materials characterization

Thermogravimetric analysis (TGA) of polylactic acid (PLA) material distinctly demonstrates its thermal degradation characteristics and thermal stability. Figure 4 illustrates that the thermal degradation of PLA occurs over a single main degradation region. The initiation of weight loss correlates with the dissociation of PLA polymer chains and the evaporation of low molecular weight constituents at about 290 °C. This temperature signifies the thermal stability limit of PLA and serves as a crucial reference for establishing the material's operational temperature [20]. The degradation process continues until around 398 °C, signifying that a substantial portion of PLA decomposes into carbon residue, necessitating the optimization of PLA's thermal

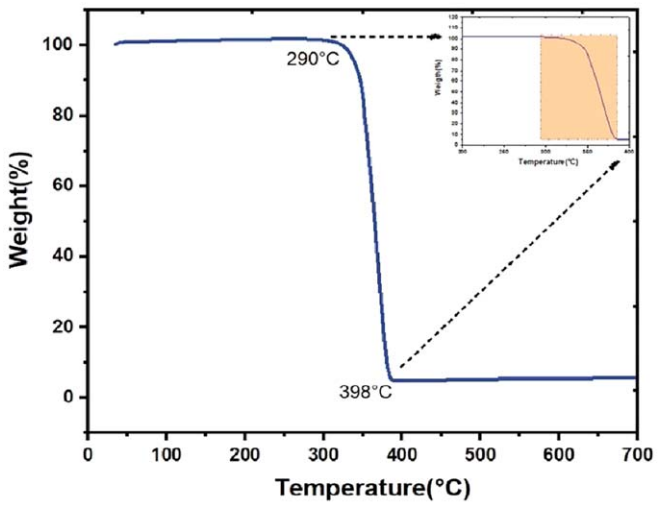

Figure 4. Thermogravimetric analysis of PLA.

Table 4. Summary of the experimental runs.

Run	Levels	
1	1.0 mm	0.2 mm
2	1.0 mm	0.4 mm
3	1.0 mm	0.6 mm
4	1.5 mm	0.2 mm
5	1.5 mm	0.4 mm
6	1.5 mm	0.6 mm
7	2.0 mm	0.2 mm
8	2.0 mm	0.4 mm
9	2.0 mm	0.6 mm

characteristics for various processing and application settings [21]. The analysis of TGA data in conjunction with current literature verifies that the degrading characteristics of PLA are often affected by variables like production methods, crystallinity levels, and the incorporation of additives. This situation is consistent with the TGA data from this study, which demonstrates a degradation temperature range of 290–398 °C, supporting the existing knowledge of PLA's thermal resilience in polymer composites and diverse applications [22].

Figures 5(a) and (b) illustrates the XRD examination of carbon fiber (CF) and polylactic acid (PLA) respectively. The XRD pattern seen in the figure indicates that carbon fiber has an amorphous structure. The graph displays a wide, low-intensity peak at around 20–25°(2θ), indicating an amorphous carbon structure. This peak signifies the irregular and non-graphitized regions of the carbon fiber. The amorphous peak arises from the inadequate graphitization of the polymers, such as polyacrylonitrile (PAN), used in carbon fiber manufacturing. Nonetheless, the lack of pronounced peaks at 2θ values of 40° and higher suggests that the graphitized [23].

Figure 5(b) shows the XRD diffractogram of a PLA (polylactic acid) sample. There is a regular reflection from a crystalline structure at the 2θ angle, where the graph shows a prominent peak, while broad and weak signals indicate the presence of an amorphous structure. PLA is generally a semi-crystalline polymer, so it can exhibit the characteristics of both crystalline and amorphous phases. The prominent peak belongs to the crystalline regions of PLA and is approximately found between 16° and 25°. This peak indicates the existence of organized molecular structures inside the polymer, typical of semi-crystalline substances [24].

The SEM pictures in figure 6 provide a detailed depiction of the microstructural morphology of the carbon fibers. The first picture, captured at 500X magnification, illustrates the overall organization and surface properties of the fibers. The fibers have a consistent shape and are aligned parallel to one another. This configuration is essential for enhancing the mechanical characteristics of carbon fibers, including tensile strength. Furthermore, little imperfections seen on the surface may suggest potential surface treatments or material flaws in the production process [25].

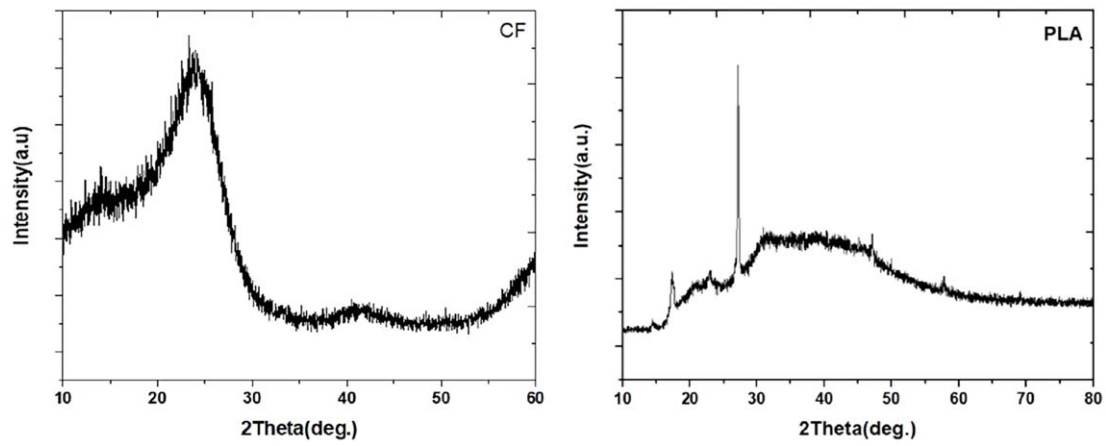

Figure 5. XRD analysis of carbon fiber and PLA.

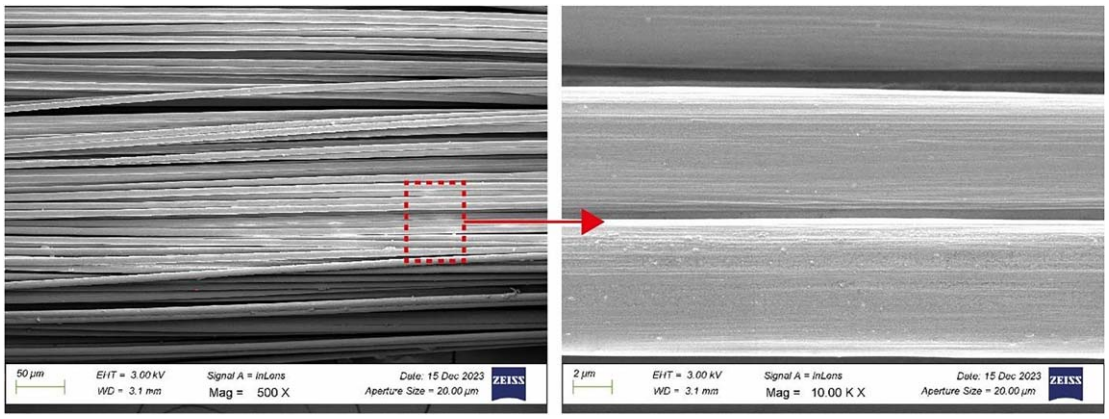

Figure 6. SEM analysis of carbon fiber.

3.2. Composite characterization

Cross-sectional stereo and optical microscope images (top and bottom portion of each image respectively) are shown in figures 7(a)–(d) for 2_06, 2_02, 1_06 and 1_02 respectively. As seen in figure 7, in case of high layer thickness, the fibers were not arranged uniformly on top of each other. On the contrary, a relatively uniform fiber arrangement was observed with decreasing layer thickness. The fibers were arranged on top of each other representing a more linear line. Fibers were deposited closer to each other with both decreasing layer thickness and line width values. The general appearance of cross-sectional profile of fibers became elliptical with decreasing layer thickness. Although most of the fibers tended to be located on the top-lateral sides of the deposited lines rather than being centered, more centrally positioned fibers which resemble an elongated rectangle were observed. In addition, with decreasing layer thickness and line width, cross-sectional profiles of some deposited fibers were affected and changed by printing adjacent lines.

The calculated fiber volume fractions of composites printed with various printing parameters are given in table 5. As clearly seen from the results (see table 5), with decreasing layer thickness and line width values, there was a significant increase in the fiber volume fraction of the composites, which is in agreement with the cross-sectional examination results. With decreasing line width and layer thickness values from 2 mm and 0.6 mm to 1 mm and 0.2 mm, respectively, the fiber volume fraction values increased from 5.41 vol% to 39.06 vol%. Kuznetsov *et al* [26] stated that the cross-sectional shape of deposited lines changed from a circle to an elongated rectangle depending on the decreasing layer thickness. It is also clear that an increase in the number of deposited lines per unit area was observed. In this study, since each printed line contains 1k carbon fiber reinforcement, an increase in the amount of carbon fiber per unit area was observed with decreasing layer thickness and line width values.

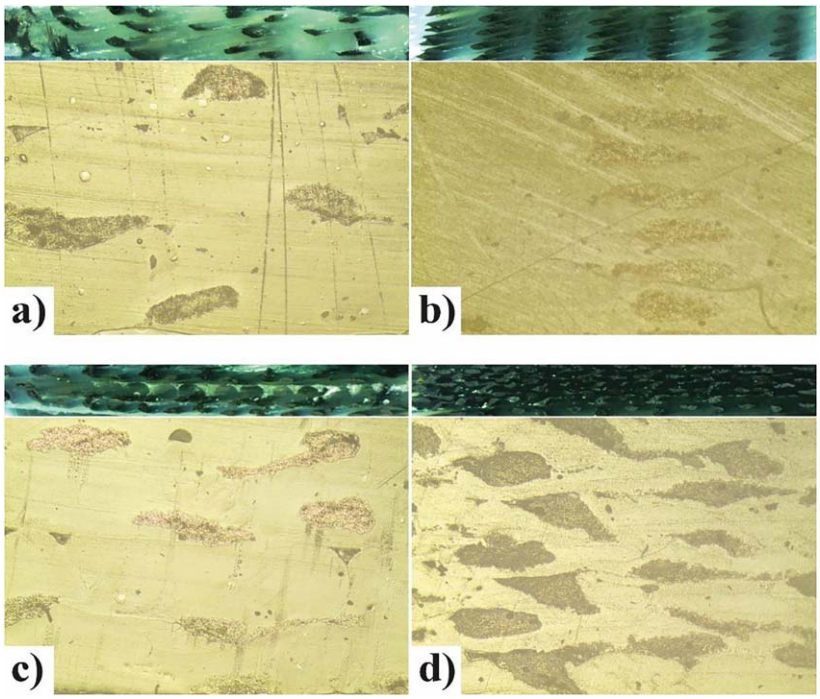

Figure 7. Stereo and optical cross-sectional images of (a) 2_06, (b) 2_02, (c) 1_06, and (d) 1_02.

Table 5. The calculated fiber volume fractions of composites.

Specimen	Fiber volume fraction (%)
2_06	5.41
2_04	8.91
2_02	19.35
1.5_06	7.19
1.5_04	11.82
1.5_02	25.67
1_06	10.91
1_04	17.96
1_02	39.06

3.3. Tensile test results

The mechanical performance of PLA-CFRP composites fabricated by the FFF method is significantly influenced by key printing parameters, particularly line width and layer thickness. These parameters directly impact fiber alignment, interlayer adhesion, and void formation, all of which are critical in determining the tensile properties of the printed composites [27]. In this study, the tensile strength values obtained under varying line width and layer thickness conditions exhibit distinct trends, demonstrating the importance of process optimization.

The results indicate that a narrower line width (1.0 mm) consistently yields higher tensile strength values, with a maximum of 291.3 MPa at 0.2 mm layer thickness (Young's modulus of 5.3 GPa). This can be attributed to improved fiber continuity and stronger bonding at the fiber-matrix interface. As the line width increases to 1.5 mm and 2.0 mm, a notable decline in tensile strength is observed, with the lowest value of 102.0 MPa recorded for a 2.0 mm line width and 0.6 mm layer thickness (Young's modulus of 4.5 GPa). The reduction in mechanical performance at larger line widths is likely due to decreased bonding efficiency between adjacent layers and potential misalignment of continuous fibers. These findings are consistent with those reported by Dou *et al* [8], who stated that the tensile mechanical properties of CFRP composites gradually decrease with increasing layer thickness and extrusion width. They further demonstrated that at an extrusion width of 0.86 mm, the tensile strength reached a maximum of 226.60 MPa, respectively, whereas an extrusion width of 1.5 mm resulted in the lowest value of 152.41 MPa. This suggests that optimizing extrusion width and layer thickness is crucial for enhancing the mechanical performance of printed composites by ensuring proper fiber alignment and interlayer adhesion.

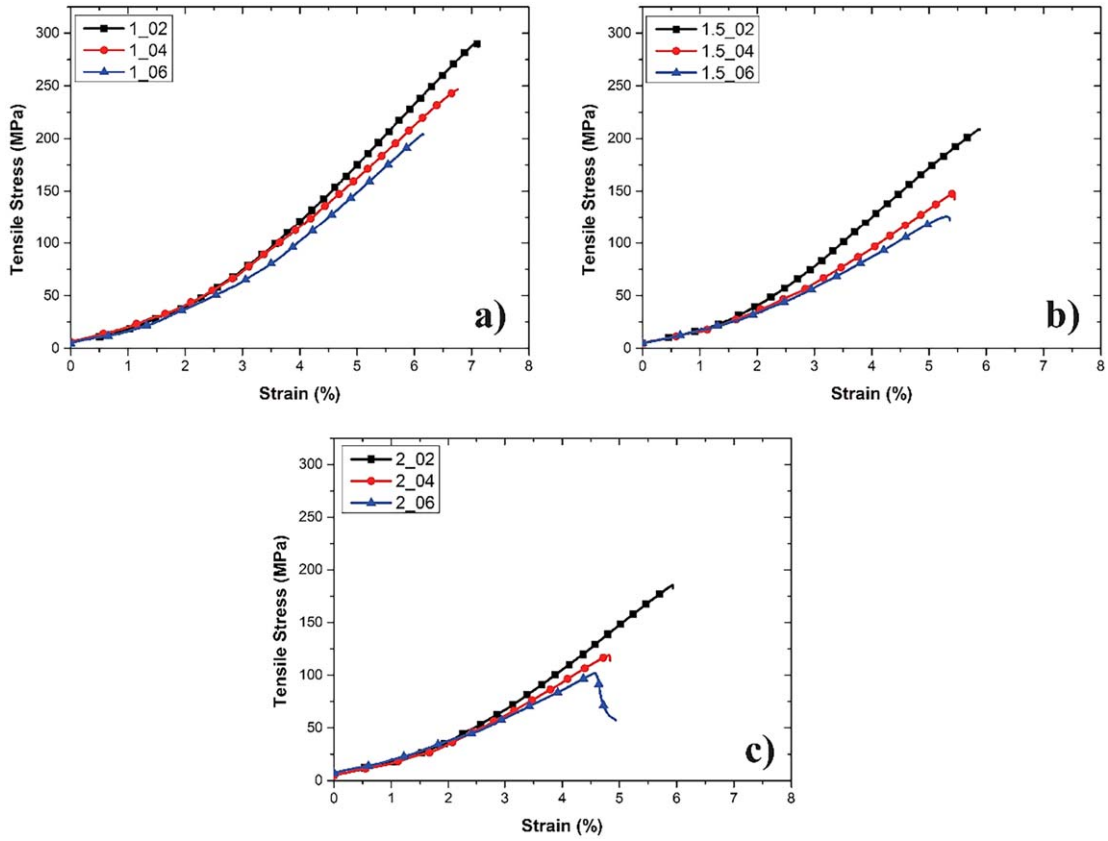

Figure 8. Tensile test results of CFRP composites, (a) 1_02, 1_04, 1_06, (b)1.5_02, 1.5_04, 1.5_0.6, (c) 2_02, 2_04, 2_06.

A similar trend is observed for layer thickness, where thinner layers (0.2 mm) result in higher tensile strength, particularly for 1.0 mm line width samples. The superior performance at lower layer thicknesses can be attributed to better fusion between layers and reduced porosity, which enhances stress transfer along the composite structure. Conversely, increasing the layer thickness to 0.6 mm leads to a progressive decline in tensile strength across all line width configurations. This decline can be linked to the presence of more interfacial defects, increased layer waviness, and lower bonding efficiency, which collectively degrade the mechanical integrity of the printed parts. This observation aligns with the findings of Vatandas *et al* [28], who stated that the primary factors contributing to the inferior mechanical properties of additively manufactured composites include inadequate interlayer adhesion, structural defects such as voids and pores, non-uniform fiber-polymer distribution, and a relatively low fiber volume fraction. These underlying mechanisms further highlight the crucial role of optimizing layer thickness to minimize defects and enhance the overall mechanical performance of the printed components.

The combined effect of line width and layer thickness reveals an optimal processing window where a line width of 1.0 mm and a layer thickness of 0.2 mm provide the highest tensile strength. This suggests that minimizing the deposited material's cross-sectional area enhances adhesion and fiber alignment, thereby improving mechanical performance. However, larger line widths and higher layer thickness compromise these benefits, leading to structural weaknesses. These findings are further supported by microstructural images, which illustrate variations in fiber distribution, interlayer bonding, and void formation under different process conditions. The tensile test results are presented in figure 8, illustrating the variations in tensile strength under different line width and layer thickness conditions

Fracture surfaces of composites labeled 2_06, 2_02, 1_06 and 1_02 are shown in figures 9(a)–(d). The common point in all figures is that the penetration of the PLA matrix into the carbon fiber tow was quite limited. Fibers were detached from the matrix and gaps between damaged fibers and matrix can be clearly seen.

The presence of relatively long fibers along the cross-section of the composite is an indication of pull-out due to the weak fiber-matrix interfacial bonding. Zhuo *et al* indicated that the nozzle impregnation method suffers from insufficient impregnation of thermoplastic matrix into the reinforcement fiber bundle because, fiber and melt of thermoplastic matrix are in contact along nozzle which has relatively short distances [29]. Similar results were observed in this study as seen in figures. Relatively enhanced impregnation of polymer into fibers was observed ass seen in figures 9(b) and (d) by decreasing layer thickness from 0.6 mm to 0.2 mm. In this thin

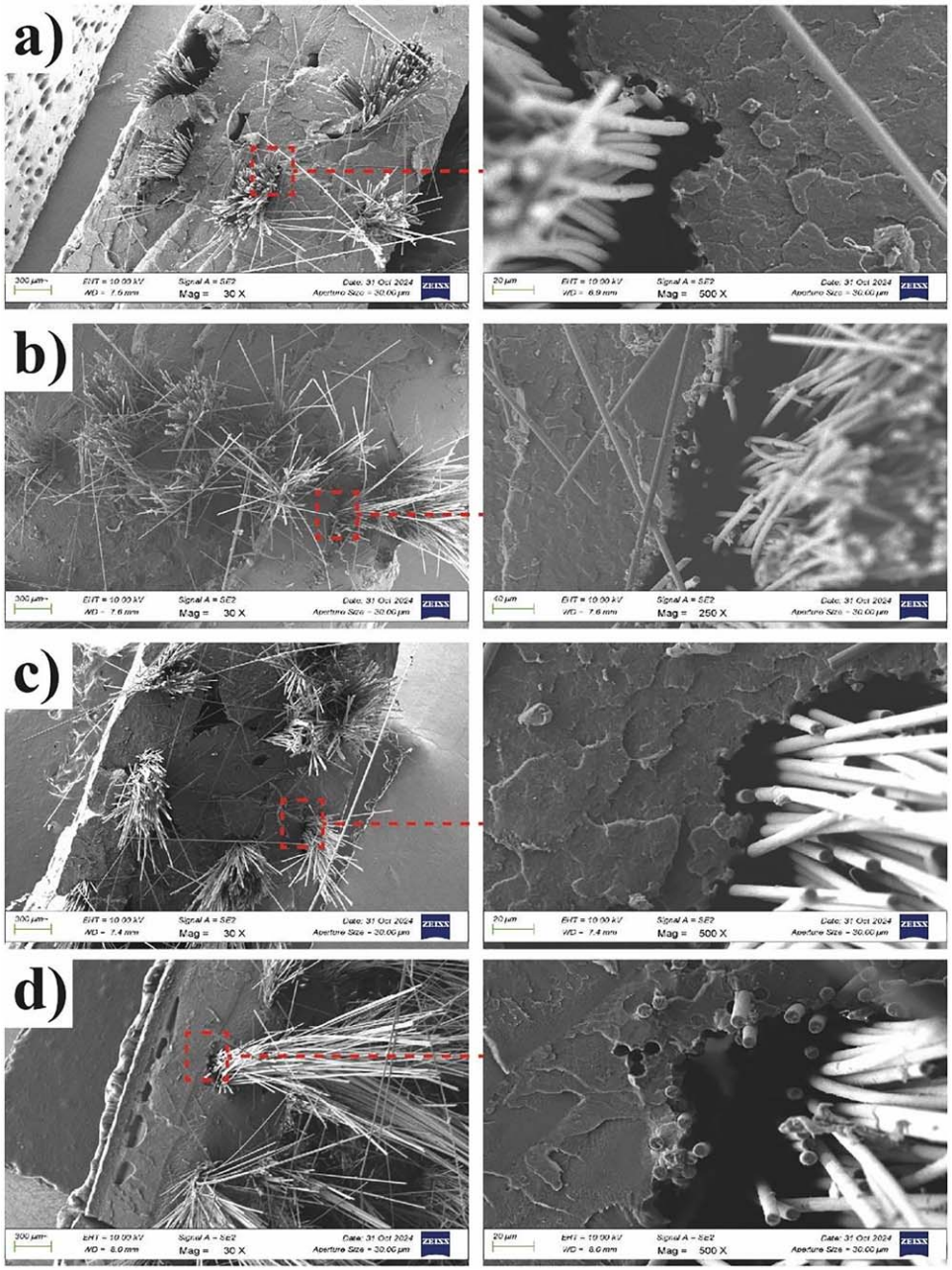

Figure 9. Fracture surface images of (a) 2_06, (b) 2_02, (c) 1_06 and (d) 1_02.

impregnation sections fibers were still attached to the PLA matrix and the fracture of these fibers occurred near the surface. Besides insufficient impregnation derived gaps, voids between deposited lines were also observed which is common for 3D printing.

It should be noted that the rounded nozzle tip is one of the most important factors for successful 3D printing of CFRP composites especially at low layer thickness values. At low layer thickness values, the direction of the carbon fiber changes up to 90° after leaving the nozzle mouth. In case of using a nozzle with a non-rounded tip, the nozzle tends to cut the fiber rather than extrude. Zhang *et al* indicated that the traction force on the deposited fiber increases with decreasing layer thickness values [30]. And the breakage of carbon fiber was observed which may strongly affect the mechanical properties of composites.

3.4. Surface roughness results

The surface roughness (Ra) values obtained from the fabricated continuous carbon fiber-reinforced composites demonstrate a clear dependence on the selected line width and layer thickness parameters. The variations in surface roughness (Ra) with respect to line width and layer thickness are illustrated in figure 10, while the measured Ra values for different parameter configurations are presented in table 6. The data clearly illustrates

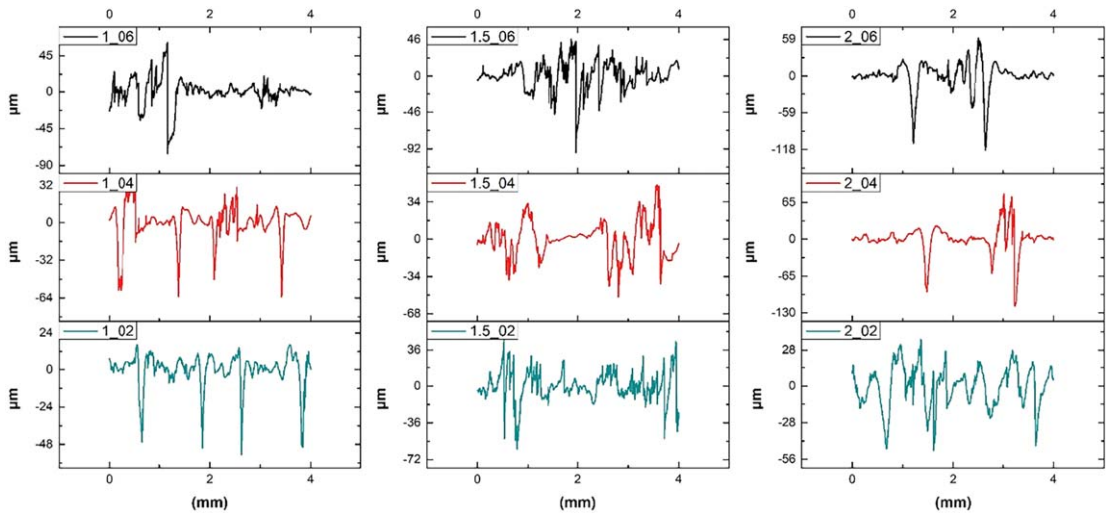

Figure 10. Surface roughness variations for composites.

Table 6. Surface roughness (R_a) results for composites.

Line width (mm)	Layer thickness (mm)	Ra (μm)
1.0	0.2	6.675
1.0	0.4	9.175
1.0	0.6	9.864
1,50	0.2	10.275
1,50	0.4	12.123
1,50	0.6	12.774
2.0	0.2	12.327
2.0	0.4	12.546
2.0	0.6	13.504

that increasing both parameters results in higher Ra values, highlighting the impact of layer deposition characteristics on surface quality. The results indicate that both process parameters significantly influence the surface quality of the printed composites, aligning well with observations reported in the literature on FDM-printed polymer composites [31, 32].

As the line width increases from 1.0 mm to 2.0 mm, a notable rise in surface roughness is observed. The lowest Ra value of 6.675 μm was recorded at 1.0 mm line width and 0.2 mm layer thickness, while the highest roughness of 13.504 μm was obtained at 2.0 mm line width and 0.6 mm layer thickness. This increase in roughness with wider extrusion paths can be attributed to higher material flow rates, which may lead to extrusion irregularities and surface waviness. Moreover, at larger line widths, overlapping inconsistencies between adjacent deposition tracks become more pronounced, further contributing to increased roughness. These findings are consistent with previous studies, which have demonstrated that excessive line width can reduce surface quality due to uneven deposition and poor bonding along the layer interfaces [31]. A direct correlation between layer thickness and surface roughness is also evident. At a fixed line width, increasing the layer thickness from 0.2 mm to 0.6 mm results in a higher Ra value. This trend is particularly notable for the 1.5 mm and 2.0 mm line width configurations, where roughness increases from 10.275 μm to 12.774 μm and from 12.327 μm to 13.504 μm, respectively. The rise in roughness with increasing layer thickness is primarily attributed to the stair-stepping effect, which becomes more prominent as the layer height increases. Thicker layers reduce the number of deposited layers, thereby reducing surface resolution and creating more pronounced layer boundaries. Similar trends have been reported in prior research, where a reduction in layer thickness was shown to improve surface smoothness due to better contour definition and minimized interlayer gaps [32]. These findings emphasize the need for parameter optimization in FFF-based composite printing, particularly when surface smoothness is a critical requirement for mechanical performance and functional applications.

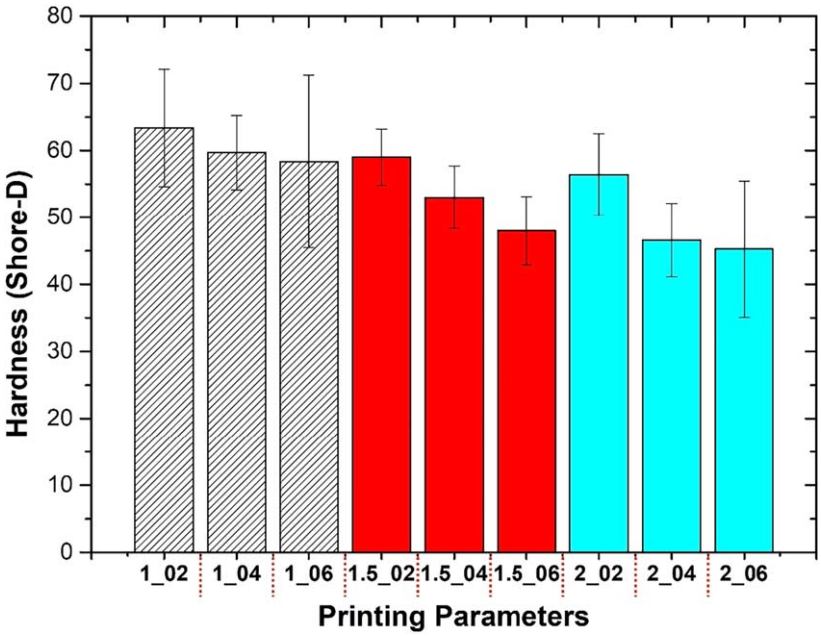

Figure 11. Hardness test results.

Table 7. The signal-to-noise (S/N) ratio values for tensile test results.

Run	S/N ratio
1	49.28
2	47.83
3	46.19
4	46.40
5	43.43
6	42.00
7	45.36
8	41.50
9	40.17

3.5. Hardness test results

The results indicate that line width and layer thickness significantly influence Shore D hardness in FFF-printed PLA-CFRP composites (see figure 11). Narrower line widths (1.0 mm) and lower layer thicknesses (0.2 mm) resulted in the highest hardness values (63.33 Shore D), attributed to improved fiber-matrix interaction and reduced void formation. Conversely, increasing line width to 2.0 mm and layer thickness to 0.6 mm led to a notable decrease in hardness (45.25 Shore D), likely due to weakened interlayer bonding and increased porosity. These findings highlight the critical role of process optimization in achieving enhanced mechanical performance in additively manufactured composites.

3.6. Taguchi analysis results

The evaluation of the signal-to-noise (S/N) ratio for different experimental conditions provides critical insights into the optimization of process parameters for PLA-CFRP composites fabricated using FFF method. As shown in table 7, the highest S/N ratio (49.28) was obtained in Run 1, indicating that this parameter combination yielded the most consistent and highest tensile strength. Conversely, Run 9 exhibited the lowest S/N ratio (40.17), suggesting that the corresponding process conditions led to increased variability and lower mechanical performance.

The observed trend highlights that process optimization plays a crucial role in enhancing mechanical properties. The decline in S/N ratios across some runs suggests a decrease in interlayer adhesion, fiber misalignment, and the presence of microstructural defects at suboptimal parameter settings. Higher S/N ratios indicate reduced variability in mechanical properties, ensuring that the selected process parameters lead to improved tensile performance with greater reliability. The results demonstrate that optimized layer thickness

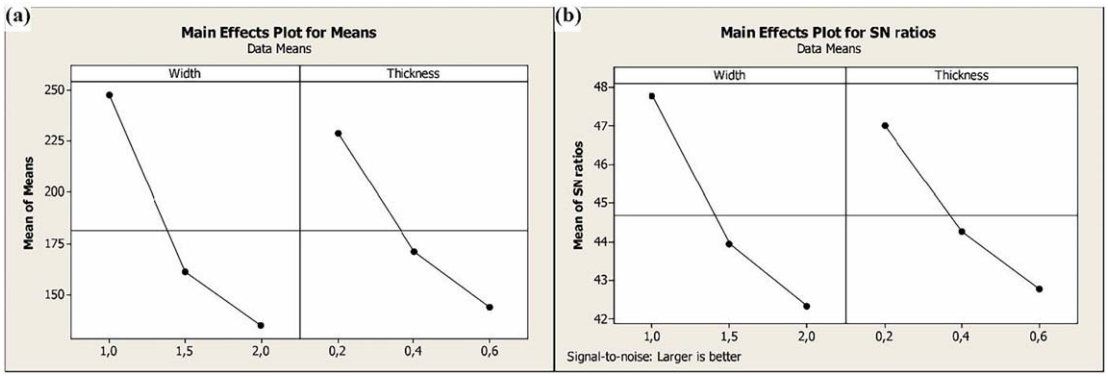

Figure 12. (a) Main effects plots for S/N ratios for composites, (b) Mean tensile strength values for composites.

Table 8. Statistical analysis results for composites.

	F-value	p-value	Contribution (%)	R^2	R^2 (adjusted)
Line width	45.1341	0.0005	58.6534		
Layer thickness	25.8164	0.0022	33.5493		
Residual			7.7972		
				0.92	0.91

and line width combinations enhance fiber-matrix interaction, thereby contributing to superior mechanical integrity.

To further quantify the influence of line width and layer thickness on tensile strength, an Analysis of Variance (ANOVA) was conducted, and the results are presented in table 8. The line width was identified as the most influential parameter, with an F-value of 45.1341 and a contribution percentage of 58.65%. This finding indicates that line width significantly impacts fiber continuity, interlayer adhesion, and void formation, all of which are critical determinants of tensile performance. A narrower line width allows for better fiber orientation and stronger bonding, whereas an increase in line width may lead to discontinuities and weaker mechanical properties [33].

The layer thickness exhibited the second highest contribution (33.55%), with an F-value of 25.8164, confirming its substantial effect on mechanical performance. Thinner layers enhance adhesion between printed layers, minimize porosity, and improve stress transfer throughout the composite structure, thereby increasing tensile strength. In contrast, thicker layers result in insufficient bonding, increased layer waviness, and microstructural inhomogeneities, all of which reduce mechanical integrity. The residual contribution was found to be only 7.80%, indicating that the selected process parameters account for the majority of the variability in tensile performance. This relatively low residual error validates the effectiveness of the Taguchi method in optimizing process parameters and ensuring reproducible mechanical properties.

Figures 12(a), (b) present the main effects plots for the S/N ratios and mean tensile strength values, respectively, offering a detailed assessment of the influence of line width and layer thickness on the mechanical behavior of PLA-CFRP composites.

4. Discussion

When literature studies are examined, the tensile strengths of continuous carbon fiber reinforced PLA matrix composites vary considerably. Results ranging from 650 MPa to 72.3 MPa were reported regarding tensile strength values. The results varied depending on the carbon fiber, printing parameters, reinforcement fraction, and method (nozzle-impregnation or pre-impregnated fiber). The tensile strength values obtained in the study are given in table 9 in comparison with various literature results.

The surface plot illustrating the tensile test results is presented in figure 13, providing a comprehensive visualization of the relationship between process parameters and mechanical performance. This graphical representation enables a clearer understanding of how variations in line width and layer thickness influence tensile strength, highlighting the optimal parameter combinations that enhance composite performance. The

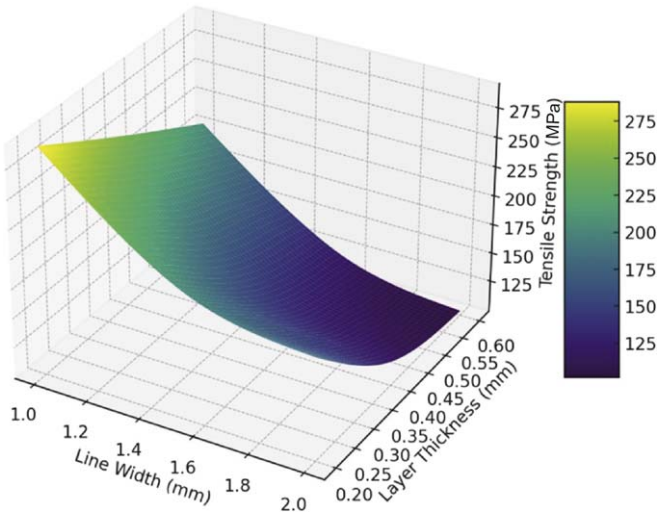

Figure 13. Surface plot of tensile test results for composites.

Table 9. Tensile strength values of various CFRP composites.

Matrix	Reinforcement	Fiber volume fraction (%)	Tensile strength (MPa)	References
PLA	Carbon fiber	22.7	243.53	[8]
PLA	Carbon fiber	6.6	185.2 ± 24.6	[34]
PLA	Carbon fiber	—	277.11 ± 4.76	[35]
PLA	Carbon fiber	—	245.40 ± 0.14	[36]
PLA	Carbon fiber	27	650	[30]
PLA	Carbon fiber	35.7	341	[37]
PLA	Carbon fiber	7.5	72.3	[38]
PLA	Carbon fiber	—	165	[39]
PLA	Carbon fiber	39.06	291.3	This study

contour variations depicted in the plot offer valuable insights into the effects of process-induced defects, fiber alignment, and interlayer bonding on the overall structural integrity of the printed composites.

5. Conclusion

This study investigated the effect of 3D printing parameters, particularly line width and layer thickness, on the tensile properties of PLA-CFRP composites fabricated using the FFF method. The application of the Taguchi method enabled a systematic analysis and optimization of these parameters, providing a structured approach to improving the mechanical performance of the printed composites.

Line width was identified as the most influential parameter, with an ANOVA contribution of 58.65%, indicating that a narrower line width (1.0 mm) significantly enhances tensile strength by improving fiber alignment and interlayer adhesion.

Layer thickness also played a critical role, contributing 33.55% to mechanical performance. Thinner layers (0.2 mm) resulted in stronger interlayer bonding and reduced porosity, leading to higher tensile strength.

Microstructural analysis revealed that fiber misalignment and void formation increased with larger line widths and thicker layers, negatively impacting the composite's structural integrity.

The highest tensile strength (291.3 MPa) was achieved at a line width of 1.0 mm and a layer thickness of 0.2 mm, demonstrating an optimal process window for FFF-printed CFRP composites.

The findings of this study contribute to the advancement of aerospace, automotive, and structural engineering applications, where lightweight and high-strength composites are essential. The ability to fine-tune process parameters enables the fabrication of high-performance composite materials, improving efficiency and broadening their industrial applicability.

Future studies should explore the effects of additional process parameters, such as printing speed and nozzle temperature, to further optimize mechanical performance. Investigating fiber orientation and stacking sequences could provide deeper insights into their role in tensile properties and interlayer bonding.

Acknowledgments

We would like to thank Balıkesir University for providing open access to the article with the read and publish agreement.

Data availability statement

All data that support the findings of this study are included within the article (and any supplementary files).

Ethical statement

The authors declare that there are no possible conflicts of interest or competing interests.

ORCID iDs

Fidan Bilir Kilinc https://orcid.org/0009-0001-9917-6465
Turker Turkoglu https://orcid.org/0000-0002-0499-9363
Saadet Guler https://orcid.org/0000-0001-9656-342X
Ahmet Cagri Kilinc https://orcid.org/0000-0003-1705-5676

References

[1] Röver T, Kuehne M, Bischop F, Clague L, Bossen B and Emmelmann C 2023 Design and numerical assessment of an additively manufactured schwarz diamond triply periodic minimal surface fluid-fluid heat exchanger *J. Laser Appl.* **35** 042071
[2] Mengesha Medibew T 2022 A comprehensive review on the optimization of the fused deposition modeling process parameter for better tensile strength of PLA-printed parts *Adv. Mater. Sci. Eng.* **2022** 1–11
[3] El Essawi B, Abdallah S, Ali S, Nassir Abdo Mohammed A, Susantyoko R A and Pervaiz S 2024 Optimization of infill density, fiber angle, carbon fiber layer position in 3D printed continuous carbon-fiber reinforced nylon composite *Results Eng.* **21** 101926
[4] Sanei S H R and Popescu D 2020 3d-printed carbon fiber reinforced polymer composites: a systematic review *J. Compos. Sci.* **4** 1–23
[5] Zhu W, Li S, Long H, Dong S, Wang K and Peng Y 2025 Simulation analysis and optimization of 3D printed continuous carbon fiber reinforced composites *Compos. Struct.* **355** 118840
[6] Safari F, Kami A and Abedini V 2022 3D printing of continuous fiber reinforced composites: a review of the processing, pre- and post-processing effects on mechanical properties *Polym. Polym. Compos.* **30** 1–26
[7] Thirugnanasamabandam A, Subramaniyan M, Prabhu B and Ramachandran K 2024 Development and comprehensive investigation on PLA/carbon fiber reinforced PLA based structurally alternate layered polymer composites *J. Ind. Eng. Chem.* **136** 248–57
[8] Dou H, Cheng Y, Ye W, Zhang D, Li J, Miao Z and Rudykh S 2020 Effect of process parameters on tensile mechanical properties of 3D printing continuous carbon fiber-reinforced PLA composites *Materials* **13** 3850
[9] Jatti V S, Sapre M S, Jatti A V, Khedkar N K and Jatti V S 2022 Mechanical properties of 3D-printed components using fused deposition modeling: optimization using the desirability approach and machine learning regressor *Appl. Syst. Innov.* **5** 1–15
[10] Ogaili A A F, Basem A, Kadhim M S, Al-Sharify Z T, Jaber A A, Njim E K, Al-Haddad L A, Hamzah M N and Al-Ameen E S 2024 The effect of chopped carbon fibers on the mechanical properties and fracture toughness of 3D-printed PLA parts: an experimental and simulation study *J. Compos. Sci.* **8** 273
[11] Rouhi Moghanlou M, Azizian-Farsani E, Mahmoudi A and Khonsari M M 2024 Optimization of FDM parameters for enhanced mechanical properties of chopped carbon fiber-reinforced polymer composites *Prog. Addit. Manuf* **10** 2073–88
[12] Petcharat N, Wiangkham A, Pichitkul A, Tantrairatn S, Aengchuan P, Bureerat S, Banpap S, Khunthongplatprasert P and Ariyarit A 2023 The multi-objective optimization of material properties of 3D print onyx/carbon fiber composites via surrogate model *Mater. Today Commun.* **37** 1–10
[13] Ponsuriyaprakash S, Udhayakumar P and Pandiyarajan R 2022 Experimental investigation of ABS matrix and cellulose fiber reinforced polymer composite materials *J. Nat. Fibers* **19** 3241–52
[14] Yu W, Wang X, Yin X, Ferraris E and Zhang J 2023 The effects of thermal annealing on the performance of material extrusion 3D printed polymer parts *Mater. Des.* **226** 111687
[15] Sethu S, Kalimuthu M, Nagarajan R, Krishnan K, Mohammad F and Arul Kumar M 2024 Hybrid fabrication and characterization of biocompatible Bamboo/PLA composites *J. Mater. Res. Technol.* **29** 2656–66
[16] Prajapati A R, Dave H K and Raval H K 2023 Impact energy absorption and fracture mechanism of FFF made fiberglass reinforced polymer composites *Rapid Prototyp. J.* **29** 275–87
[17] Waterbury M C and Drzal L T 1989 Determination of fiber volume fractions by optical numeric volume fraction analysis *J. Reinf. Plast. Compos.* **8** 627–36
[18] Morales C N, Claure G, Álvarez J and Nanni A 2020 Evaluation of fiber content in GFRP bars using digital image processing *Composites B* **200** 108307
[19] Hisam M W, Dar A A, Elrasheed M O, Khan M S, Gera R and Azad I 2024 The versatility of the taguchi method: optimizing experiments across diverse disciplines *J. Stat. Theory Appl.* **23** 365–89

[20] Gumowska A, Robles E, Bikoro A, Wronka A and Kowaluk G 2022 Selected properties of bio-based layered hybrid composites with biopolymer blends for structural applications *Polymers* **14** 4393
[21] Cordeiro E S, Luna C B B, da Silva R A, Ramos Wellen R M, de Carvalho L H and de Souza D D 2023 On the production of poly(lactic acid) (PLA) compounds with metallic stearates based on zinc, magnesium and cobalt. Investigation of torque rheometry and thermal properties *J. Elastomers Plast.* **55** 805–21
[22] Li H, Wu Z, Xue F, Bai J and Chu C 2018 Influence of equal channel angular pressing on the properties of polylactic acid *Polym. Eng. Sci.* **58** 665–72
[23] Yılmaz Y, Çallıoğlu H and Balbay A 2022 Investigation of quasi-static crushing and energy absorption behaviors of carbon nanotube reinforced glass fiber/epoxy and carbon fiber/epoxy composite tubular structures *Pamukkale Univ. J. Eng. Sci.* **28** 81–90
[24] Ranjbar M, Pardakhty A, Tahmipour B and Mohamadzadeh I 2019 Novel CaO/polylactic acid nanoscaffold as dental resin nanocomposites and the investigation of physicochemical properties *Luminescence* **34** 360–7
[25] Feraboli P, Kawakami H, Wade B, Gasco F, DeOto L and Masini A 2012 Recyclability and reutilization of carbon fiber fabric/epoxy composites *J. Compos. Mater.* **46** 1459–73
[26] Kuznetsov V E, Solonin A N, Urzhumtsev O D, Schilling R and Tavitov A G 2018 Strength of PLA components fabricated with fused deposition technology using a desktop 3D printer as a function of geometrical parameters of the process *Polymers* **10** 1–11
[27] Kilinc F B, Bozaci E, Kilinc A C and Turkoglu T 2025 Effect of atmospheric plasma treatment on mechanical properties of 3D-printed continuous aramid fiber/PLA composites *Polymers* **17** 397
[28] Barış Vatandaş B, Uşun A, Yıldız N, Şimşek C, Necati Cora Ö, Aslan M and Gümrük R 2023 Additive manufacturing of PEEK-based continuous fiber reinforced thermoplastic composites with high mechanical properties *Composites* A **167** 107434
[29] Zhuo P, Li S, Ashcroft I A and Jones A I 2021 Material extrusion additive manufacturing of continuous fibre reinforced polymer matrix composites: a review and outlook *Composites* B **224** 109143
[30] Zhang Z, Long Y, Yang Z, Fu K and Li Y 2022 An investigation into printing pressure of 3D printed continuous carbon fiber reinforced composites *Composites* A **162** 107162
[31] Mani M, Karthikeyan A G, Kalaiselvan K, Muthusamy P and Muruganandhan P 2022 Optimization of FDM 3-D printer process parameters for surface roughness and mechanical properties using PLA material *Mater. Today Proc.* **66** 1926–31
[32] Kim M K, Lee I H and Kim H-C 2018 Effect of fabrication parameters on surface roughness of FDM parts *Int. J. Precis. Eng. Manuf.* **19** 137–42
[33] Turkoglu T and Kilinc A C 2025 Optimization of process parameters for steel wire-reinforced polylactic acid composites produced by additive manufacturing *Polymers* **17** 624
[34] Matsuzaki R, Ueda M, Namiki M, Jeong T-K, Asahara H, Horiguchi K, Nakamura T, Todoroki A and Hirano Y 2016 Three-dimensional printing of continuous-fiber composites by in-nozzle impregnation *Sci. Rep.* **6** 23058
[35] Wang F, Zhang Z, Ning F, Wang G and Dong C 2020 A mechanistic model for tensile property of continuous carbon fiber reinforced plastic composites built by fused filament fabrication *Addit. Manuf.* **32** 101102
[36] Maqsood N and Rimašauskas M 2021 Characterization of carbon fiber reinforced PLA composites manufactured by fused deposition modeling *Compos. Part C Open Access* **4** 100112
[37] Isobe T, Tanaka T, Nomura T and Yuasa R 2018 Comparison of strength of 3D printing objects using short fiber and continuous long fiber *IOP Conf. Ser.: Mater. Sci. Eng.* **406** 012042
[38] Gür Y, Çelik S and Sakin R 2024 Tensile behaviour of continuous carbon fibre reinforced composites fabricated by a modified 3D printer *Mater. Res. Express* **11** 075305
[39] Rimašauskas M, Kuncius T and Rimašauskienė R 2019 Processing of carbon fiber for 3D printed continuous composite structures *Mater. Manuf. Process.* **34** 1528–36